energies

Article

Prediction of Blast Furnace Gas Generation Based on Bayesian Network

Zitao Wu and Dinghui Wu *

School of Internet of Things Engineering, Jiangnan University, Wuxi 214122, China
* Correspondence: wdh123@jiangnan.edu.cn; Tel.: +86-13961854865

Abstract: Due to the large fluctuation of blast furnace gas (BFG) generation and its complex production characteristics, it is difficult to accurately obtain its gas change rules. Therefore, this paper proposes a prediction method of BFG generation based on Bayesian network. First, the BFG generation data are divided according to the production rhythm of the hot blast stove, and the training event set is constructed for the two dimensions of interval generation and interval time. Then, the Bayesian network of generation and the Bayesian network of time corresponding to the two dimensions are built. Finally, the state of each prediction interval is inferred, and the results of the reasoning are mapped and combined to obtain the prediction results of the BFG generation interval combination. In the experiment part, the actual data of a large domestic iron and steel plant are used to carry out multi-group comparison experiments, and the results show that the proposed method can effectively improve the prediction accuracy.

Keywords: blast furnace gas; data division; event set construction; Bayesian network

Academic Editor: Shu Tao

Received: 3 February 2025
Revised: 22 February 2025
Accepted: 23 February 2025
Published: 28 February 2025

Citation: Wu, Z.; Wu, D. Prediction of Blast Furnace Gas Generation Based on Bayesian Network. *Energies* **2025**, *18*, 1182. https://doi.org/10.3390/en18051182

1. Introduction

BFG is a by-product of the reduction reaction of iron oxide in the blast furnace [1,2], which is an important by-product energy in the production process of iron and steel enterprises and is widely used in the production process of sintering and hot rolling, etc. [3]. The fluctuation of BFG generation affects the status of much equipment in long-process steelmaking. It is of great significance to establish an accurate prediction model of BFG generation for the energy management of enterprises.

In the literature, methods for by-product gas prediction include time series analysis [4], supervised learning [5,6], neural networks [7–9], dual-drive modeling [10,11], granularity calculations [12–15] and probabilistic inference [16–18], etc. Among them, study [4] proposes an adaptive time series model to predict each generation unit and consumption unit of by-product gas and uses the MILP optimization model to executive short-term decisions. Studies [5,6] have conducted parameter optimization of least squares support vector machine models based on genetic algorithms and online hyper-parameter optimization methods, respectively, which are suitable for real-time point prediction of generation. Studies [7,8] propose a two-stage online prediction method and an integrated model incorporating quantile regression (QR-ESNE) based on echo state network (ESN), respectively, with the former using ESN to predict the production and consumption of the BFG in the first stage, and constructing the storage tank model based on the effectors in the second stage, and the latter incorporating a Bootstrap strategy to construct the confidence interval and prediction interval of the BFG. Study [9] builds a bootstrapping reservoir computational network and uses a simultaneous parameter training method based on Bayesian linear regression, which is applicable to nonlinear time series such as BFG generation. Study [10] establishes data and knowledge dual-driven soft sensors assisted by attention mechanisms. Study [11] proposes hybrid event, mechanism, and data-driven models which combine a priori knowledge of the blast furnace to select the best prediction model for different events. Studies [12,13] are based on the approach of granularity computation—the former granularizes the industrial drive semantics and adopts the fuzzy C-mean cluster analysis method to reflect the industrial operation mode and construct the fuzzy rules for energy flow prediction, and the latter proposes the method of constructing the prediction intervals based on the granularity computation, which provides the guidance for predicting the integration of scheduling. Study [14] constructs prediction intervals based on hierarchical granularity computation and strengthens the model structure using Monte Carlo search which improves the generalization ability of the model. Study [15] proposes an approach based on adaptive granularization, which firstly divides the information granules based on the production semantics of fluctuating trends in energy data, and then proposes a synergistic conditional fuzzy clustering approach to refine the description of trend-based features. The above studies provide many ideas for predicting BFG generation, but most of the methods focus on the BFG generation itself and neglect the research on the equipment related to the BFG generation. Moreover, the changes in the state of this equipment will always affect the changes in BFG generation, so it is necessary to pay attention to their influence on the prediction of BFG generation.

Considering the multi-equipment, multi-process coupling in the steelmaking process, probabilistic inference methods such as Bayesian networks have been widely emphasized. Bayesian network-based methods are capable of modeling complex dependencies and analyzing complex systems with multivariate interactions which are widely used in long-process steelmaking processes. Study [16] proposes the idea of real-time gas dynamic scheduling, which models the probabilistic relationships described by Bayesian networks and ultimately provides scheduling solutions. Study [17] proposes the Takagi-Sugeno (T-S) fuzzy modeling method based on Bayesian block structure sparsity, and uses the variational Bayesian method for inference and solution to achieve the dynamic prediction of iron silicon content. Study [18] proposes a steam flow time series prediction model with a Bayesian echo state network designed to provide decision support for steam systems. In terms of project risk assessment, study [19] proposes a fuzzy Bayesian network based on interval V-value fuzzy sets and improved D-S evidence theory, which employs expert judgment to classify the data levels, aiming to provide a reliable risk assessment. Although the above studies on the application of Bayesian networks have not directly demonstrated the applicability to the prediction of BFG generation, their findings show its feasibility for reasoning about coupled systems. Among them, the predictions on steam and silicon content of ferro-water in long-process steelmaking demonstrated the adaptability of Bayesian networks to the complex energy data of iron and steel systems [17,18]. Research on project risk assessment has also demonstrated the feasibility of Bayesian networks for reasoning about complex systems after event-based processing [19].

Based on the above research results, and combined with the influence of key factors such as hot blast furnace energy consumption on blast furnace gas generation, this paper takes the BFG generation as the research object, and proposes a Bayesian network-based prediction method. Firstly, according to the relationship between blast furnace and its own hot blast furnace in process, the data division of BFG generation is carried out to obtain the level data. Then, in order to find the connection within and between data segments, the event set is constructed from the dimensions of interval generation and interval time, and the Bayesian networks corresponding to different dimensions are built to perform the state inference of generation. Finally, the inference results are mapped, and the mapped generation prediction intervals are combined to obtain the prediction results of generation interval combination. The results of the experimental part show that the method of this paper can meet the practical needs of prediction.

This paper is structured as follows: Section 2 analyzes the problems involved in BFG generation prediction; Section 3 describes the generation prediction method based on the Bayesian network; Section 4 compares and analyzes the experimental results to validate the effectiveness of the proposed method; and Section 5 summarizes the contents of this paper and gives an outlook.

2. Description of the Problem

In the long-process steelmaking process, the blast furnace and the hot blast furnace are two important devices that are closely related, and their synergistic efficiency has a direct impact on the quality of steelmaking. The hot blast furnace provides high-temperature air for the blast furnace to maintain a stable operation, while the hot blast furnace also needs the stable operation of the blast furnace to maintain the hot air circulation, as shown in Figure 1.

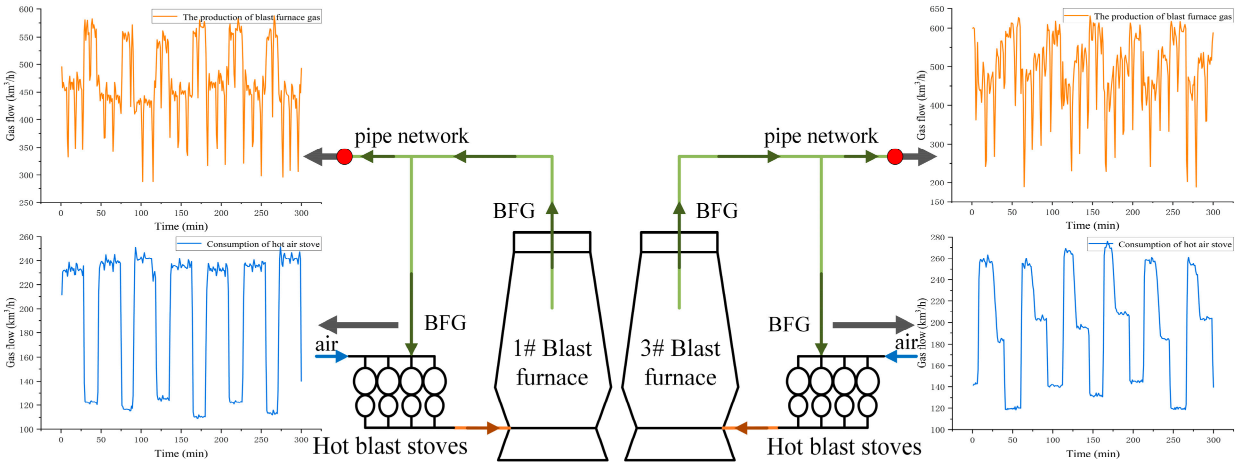

Figure 1. Relationship between the blast furnace and the hot blast stove.

At the data level, both BFG generation and its own hot blast furnace consumption during normal operation have quasi-periodic characteristics, and there are consistent fluctuations in time between BFG generation and its own hot blast furnace consumption due to the relationship between the blast furnace and the hot blast furnace in long-process steelmaking. This process relationship between blast furnace and its own hot blast furnace is very important for the prediction of BFG generation, and many methods ignore this relationship, whereas the Bayesian network based on the event concept can rely on its own structure to discover this relationship and more comprehensively predict the generation. Therefore, in this paper, based on Bayesian network theory, the knowledge extracted from the relationship between blast furnace and hot blast furnace is evented to build a network inference model of BFG generation.

3. Inference and Prediction Method of BFG Generation

Considering the influence of hot blast furnace consumption on BFG generation prediction, this paper proposes a generation prediction method based on a Bayesian network. The method can be divided into three stages. The first stage mainly carries out the data division of BFG generation as well as the construction of event set of the two dimensions of interval generation and interval time. The second stage combines the previous knowledge of the BFG generation process to construct the generation Bayesian network and time Bayesian network under two dimensions. The third stage relies on the network model to perform state inference for the prediction intervals, and maps and combines the inference results to obtain the prediction results for the generation interval combination.

3.1. Data Division and Event Set Construction

3.1.1. Data Division

Considering the difference in the fluctuation of BFG generation caused by the difference in the number of self-allocated hot blast furnaces of different blast furnaces, this section selects the representative BFG generation and its self-allocated hot blast furnace consumption data of Blast Furnace 1 and Blast Furnace 3 as the samples to be studied, and divides the data of BFG generation according to the production rhythm of hot blast furnaces.

The hot air furnace consumption sequence has multiple segments with a certain upward or downward trend, and this section sets up a window $L = [l_1, \cdots, l_m]$, $m \in N^+$ with a fixed length, and detects the trend of the data within the window through the gradual sliding of the window L in the hot air furnace consumption sequence.

Due to the small sample size of the data within each window and not meeting the conditions of normal distribution, this paper uses the Mann–Kendall test [20] to detect whether the data within the window contains a certain upward or downward trend, and the formula of the Mann–Kendall test is shown in Equations (1)–(4). Equation (1) is used to calculate the sign functions of all the different numbers within the window and the statistics of all the sign functions are obtained by Equation (2). Since all data in the window are unique, the formula for calculating the variance of the statistic is simplified to Equation (3), and since the statistic approximately follows a normal distribution, the standard normally distributed statistic of Equation (4) is established.

$$\mathrm{sgn}(l_a - l_b) = \begin{cases} 1 & l_a - l_b > 0 \\ 0 & l_a - l_b = 0 \\ -1 & l_a - l_b < 0 \end{cases} \quad (1)$$

$$Y = \sum_{b=1}^{m-1} \sum_{a=b+1}^{m} sgn(l_a - l_b) \quad (2)$$

$$Var\ (Y) = \frac{1}{18}[m(m-1)(2m+5)] \quad (3)$$

$$U = \begin{cases} \frac{Y-1}{\sqrt{Var\ (Y)}} & Y > 0 \\ 0 & Y = 0 \\ \frac{Y+1}{\sqrt{Var\ (Y)}} & Y < 0 \end{cases} \quad (4)$$

where, $a, b \in [1, m]$ and $a \neq b$.

For the window L to be tested, two hypotheses are set: the original hypothesis H_0 states that there is no certain upward or downward trend, while the alternative hypothesis H_1 states that there is a certain upward or downward trend in L. The process for testing the trend of the window L is as follows.

Step 1: Set a fixed-length window L and slide the window step by step in the consumption sequence of the hot air furnace, calculating all $\frac{m(m-1)}{2}$ symbol functions $\mathrm{sgn}(l_a - l_b)$ within the window L according to Equation (1).

Step 2: Calculate the statistic Y for window L and the variance of Y according to Equations (2) and (3).

Step 3: Since the statistic Y approximately follows a normal distribution, the standard normal distribution statistic U is established according to Formula (4) and $|U|$ is calculated.

Step 4: Set α to 0.05. If $|U| \geq U_{1-\alpha/2}$, do not accept the original hypothesis, which means that at the α confidence level, there is a certain upward or downward trend in window L. The type of trend in window L is determined by the sign of U. If $U > 0$, it is an upward trend, and if $U < 0$, it is a downward trend. If $|U| < U_{1-\alpha/2}$, accept the original hypothesis.

Step 5: Determine whether the hot air furnace consumption sequence is all detected, if complete, record the location of the median of all windows where a certain upward or downward trend exists, otherwise return to Step 1.

For all windows with certain upward or downward trends, there are cases in which the positions of the window medians are continuous in the time series, and the medians of the data segments where these median positions are consecutive are taken as the quasi-periodic cut-off points. For Blast Furnace 1, the data are divided into high and low levels according to the quasi-periodic cut-off point, as shown in Figure 2. For Blast Furnace 3, according to the quasi-periodic cut-off point, the data will be divided into high, medium and low levels, as shown in Figure 3.

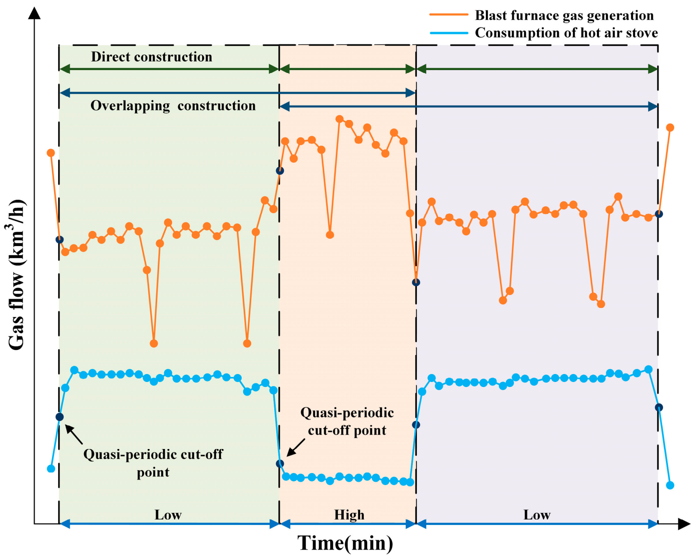

Figure 2. Data division and event set construction for Blast Furnace 1.

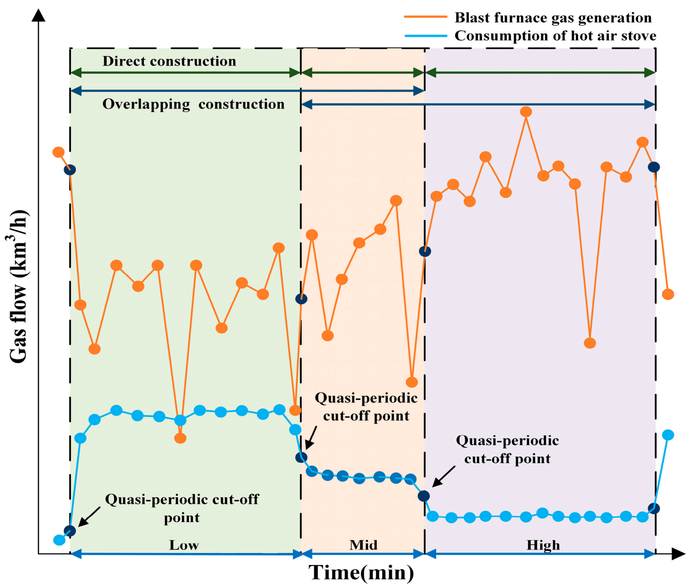

Figure 3. Data division and event set construction for Blast Furnace 3.

3.1.2. Construction of Training Event Set

The level data obtained from data division will be used to determine the intervals corresponding to each state in the training event set. Since the different ways of interval construction will lead to the differences in the training event set and the changes in the network structure, this section adopts both direct construction and overlapping construction to identify these intervals. Direct construction uses level data segments as the corresponding intervals, and overlap construction combines the time-ordered level data segments two by two, and the combined data segments are used as the corresponding intervals, as shown in Figures 2 and 3. The training event sets are constructed directly and overlapped from two dimensions of interval generation and interval time, respectively.

Denote c as 1 or 3, representing Blast Furnace 1 and Blast Furnace 3, respectively; and e as DC or OC, representing direct construction and overlapping construction, respectively. Define R_e^c as the set of generation amounts for each interval arranged in chronological order under the c blast furnace e method, and T_e^c as the set of time for each interval arranged in chronological order under the c blast furnace e method, $R_e^c = \{R_{e1}^c, R_{e2}^c, \cdots, R_{eo}^c, \cdots, R_{eh}^c\}$, $T_e^c = \{T_{e1}^c, T_{e2}^c, \cdots, T_{eo}^c, \cdots, T_{eh}^c\}$, $o \in [1, h]$, $o \in N^+$, h is the total number of intervals under the c blast furnace e method.

The statistical units of the elements in the interval time set T_e^c of Blast Furnace 1 and Blast Furnace 3 are all minutes, and the training event set is constructed on the basis of the interval time, with each state in the training event set representing the time of the interval.

The distribution of the elements in the interval generation set R_e^c of Blast Furnace 1 and Blast Furnace 3 are positively skewed, which need to be transformed by normalization to approximate the normal distribution in order to construct the training event set using the properties of the normal distribution. The skewness and kurtosis of the distribution of elements in the set are calculated by the Equations (5) and (6). Based on the skewness and kurtosis of the positively skewed distribution, it was determined that the $Box - cox$ transformation [21] of Equation (7) was used to approximate the normal distribution.

$$Skewness = \frac{\frac{1}{h}\sum\limits_{o=1}^{h}\left(R_{eo}^c - \overline{R}_e^c\right)^3}{\sigma^3} \tag{5}$$

$$Kurtosis = \frac{\frac{1}{h}\sum\limits_{o=1}^{h}\left(R_{eo}^c - \overline{R}_e^c\right)^4}{\sigma^4} - 3 \tag{6}$$

$${R_{eo}^c}^{(\lambda)} = \begin{cases} \frac{{R_{eo}^c}^{(\lambda)} - 1}{\lambda} & \lambda \neq 0 \\ \ln\left(R_{eo}^c\right) & \lambda = 0 \end{cases} \tag{7}$$

where, $Skewness$ and $Kurtosis$ denote the skewness and kurtosis, respectively, λ is the parameter of the $Box - cox$ transformation, σ is the standard deviation, and $\overline{R}_e^c$ is the mean of all the elements in the set R_e^c.

The parameter λ of the $Box - cox$ transformation of Equation (7) was determined by maximum likelihood estimation. According to the Lajda principle of normal distribution, the probability that the transformed data are distributed within three standard deviations σ is 68.27%, 95.45% and 99.73%, respectively. The interval states are set according to the approximate proportions corresponding to the data within the three standard deviations, then the training event sets of set R_e^c of Blast Furnace 1 and Blast Furnace 3 are constructed, and each state in the training event set represents the median of the corresponding interval generation in the event set.

The constructed interval generation training event set and interval time training event set are represented by Equation (8) and Equation (9), respectively.

$$R_e'^c = \{R_{e1}'^c, R_{e2}'^c, \cdots, R_{eo}'^c, \cdots, R_{eh}'^c\} \tag{8}$$

$$T_e'^c = \{T_{e1}'^c, T_{e2}'^c, \cdots, T_{eo}'^c, \cdots, T_{eh}'^c\} \tag{9}$$

where, $R_{eo}'^c$ denotes the generation state of the $o-th$ interval in chronological order under the c blast furnace e method, and $T_{eo}'^c$ denotes the time state of the $o-th$ interval in chronological order under the c blast furnace e method.

3.2. Bayesian Network Modeling

Each element in the training event set represents a kind of node's state, and this section utilizes the training event set in Section 3.1.2 to learn the structure of Bayesian networks. It is necessary to set up the Bayesian network nodes reasonably in the structure learning. Combining the training event sets $R_e'^c$ and $T_e'^c$, determine the initial connection relationship of the 8 nodes connected in chronological order. The training event sets $R_e'^c$ and $T_e'^c$ are used as inputs, and the CH scoring function is utilized to traverse the parent nodes of node X_i^c on the basis of the initial connectivity relationship, obtaining the generation network and time network of Blast Furnace 1 and Blast Furnace 3, as shown in Figure 4. Denote X as R or T, representing the generation network or the time network, respectively. The formula for the CH scoring function [22] is shown in Equation (10).

$$P(D,S) = P(S)\prod_{i=1}^{n}\prod_{j=1}^{q_i}\frac{(r_i-1)!}{(N_{ij}+r_i-1)!}\prod_{k=1}^{r_i}N_{ijk}! \tag{10}$$

where, S and D represent the network structure and the training event set, $P(S)$ is the prior probability of the network, n is the number of nodes, r_i is the number of values that node X_i^c can take, q_i is the number of combinations of values taken by the parent node of node X_i^c, N_{ijk} is the quantity of instances where the parent nodes of node X_i^c are in a certain combination of values and X_i^c takes a certain value, and N_{ij} is the number of the parent nodes of node X_i^c in a certain combination of values, $N_{ij} = \sum_{k=1}^{r_i} N_{ijk}$.

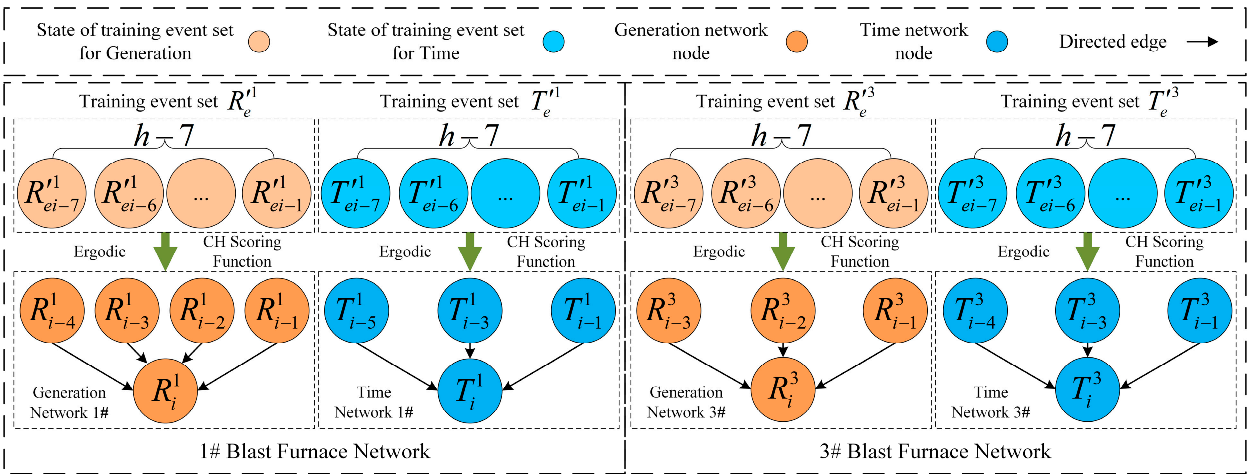

Figure 4. Network structure of Blast Furnace 1 and Blast Furnace 3 under different dimensions. (The left and right parts of the figure represent the two sets of networks used for inference in blast furnaces No. 1 and No. 3, respectively, where each column in each part represents the inference process and network structure of the generation network and the time network.).

The learning process of the Bayesian network structure is as follows. The $h-7$ group of elements in the training event sets $R_e'^c$ and $T_e'^c$ are taken as input, with each group containing eight elements, as shown in Figure 4. According to Equation (10), the parent node that most enhances the CH score is added to node X_i^c until the score is no longer improved or the maximum number of parent nodes limit is reached, and the network structure with the highest score under the CH scoring function is obtained.

The inference effect of the network structure under the two dimensions of Blast Furnace 1 and Blast Furnace 3 is compared to obtain the four sets of network structure used for state inference in this paper, as shown in Figure 4. It can be seen through Figure 4 that the differences in the network structures are attributed to the different ways of dividing the training event sets of Blast Furnace 1 and Blast Furnace 3.

3.3. State Reasoning and Mapping and Combining Reasoning Results

The network structure learned from the above process will be used for state inference in the prediction interval. The prediction event sets $R_e''^c = \left\{R_{ei-7}''^c, R_{ei-6}''^c, \cdots, R_{ei-1}''^c\right\}$ and $T_e''^c = \left\{T_{ei-7}''^c, T_{ei-6}''^c, \cdots, T_{ei-1}''^c\right\}$ used for inference are constructed based on the training event sets $R_e'^c$ and $T_e'^c$. Each element in $R_e''^c$ and $T_e''^c$ represents the state of the corresponding node at the time of inference. The prediction event sets $R_e''^c$ and $T_e''^c$ are input into the Bayesian network constructed in Section 3.2 for state inference of prediction interval, and then the inference results are mapped into prediction intervals for the generation, as shown in Figure 5.

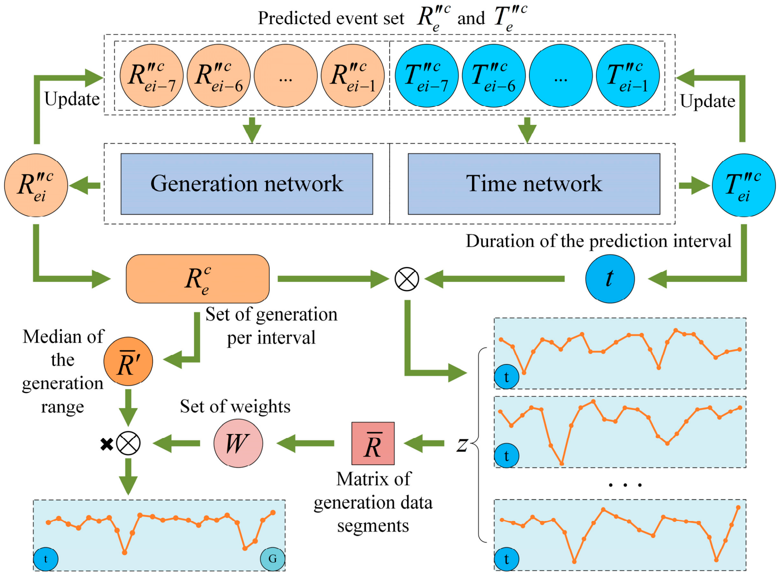

Figure 5. State Reasoning and Mapping of Reasoning Results. (The top half of the figure indicates how to obtain the two states, and the bottom half indicates how to reduce from the states to the predicted occurrence data.).

The state and expectation of the next prediction interval are obtained by inference through the expectation formula of the network conditional probability (Equation (11)).

$$E\left[\theta_{ijk}\middle|D,S\right] = \frac{N_{ijk}+1}{N_{ij}+r_i} \tag{11}$$

where, θ_{ijk} is the network conditional probability.

Regarding the generation state and the time state obtained from inference, it is necessary to treat them separately due to the different dimensions and the different way of constructing the training event sets. For the time state obtained by inference, the corresponding value of the state in set T_e^c is the time t of the prediction interval. For the generation states obtained by inference, the range of interval generation corresponding to the states can be found in the set R_e^c, and the median $\overline{R}'$ corresponding to this range is obtained. Based on the predicted interval time t, the generation data segments in set R_e^c with the same time t and the same way of constructing the interval can be found. Assuming that there are z such generation data segments, combining them into a generation data segment matrix $\overline{R}$ (Equation (12)), the set of weights W for the median of the interval generation range is calculated by Equations (13) and (14), and thus the generation prediction interval G is obtained.

$$\overline{R} = \begin{bmatrix} \overline{R}_{11} & \overline{R}_{12} & \cdots & \overline{R}_{1t} \\ \overline{R}_{21} & \overline{R}_{22} & \cdots & \overline{R}_{2t} \\ \vdots & \vdots & \ddots & \vdots \\ \overline{R}_{z1} & \overline{R}_{z2} & \cdots & \overline{R}_{zt} \end{bmatrix} \tag{12}$$

$$W_\eta = \frac{\sum\limits_{f=1}^{z} \overline{R}_{f\eta}}{\sum\limits_{f=1}^{z}\sum\limits_{g=1}^{t} \overline{R}_{fg}} \tag{13}$$

$$W = \{W_1, W_2, \cdots, W_t\} \tag{14}$$

$$G = \overline{R}' W = \{G_1, G_2, \cdots, G_t\} \tag{15}$$

where, $f \in [1, z]$, $g \in [1, t]$, $\eta \in [1, t]$ and $f, g, \eta \in N^+$.

The steps of inputting the predicted event sets $R_e^{''c}$ and $T_e^{''c}$ into the network for state inference and then mapping the inference results are as follows.

Step1: The set of predicted events $R_e^{''c}$ and $T_e^{''c}$ are used as inputs to reason about states $R_{ei}^{''c}$ and $T_{ei}^{''c}$ in the next prediction interval according to Equation (11).

Step2: Based on the corresponding values of the generation inference state $R_{ei}^{''c}$ and the time inference state $T_{ei}^{''c}$, the median $\overline{R}'$ of the generation range in the prediction interval and the time t of the prediction interval are obtained.

Step3: Search for generation data segments in set R_e^c that have the same prediction interval time t and the same interval construction to construct the generation data segment matrix $\overline{R}$ of Equation (12).

Step4: The weight matrix W of the generation prediction interval is calculated according to Equations (12)–(14), which in turn is combined with Equation (15) to calculate the generation prediction interval G at time t.

Step5: Set $i = i + 1$, return to Step1.

All generation prediction intervals G are combined in chronological order to obtain the prediction results of generation interval combinations, and the quality of the prediction results will be comparatively analyzed in Section 4.

4. Experiments and Analysis

In order to verify the validity of the method proposed in this paper, 80,000 min of BFG generation data at the same time for Blast Furnace 1 and Blast Furnace 3 are selected for the construction of the training event set and network learning, and 1400 min of data are selected for the validation of inference results.

Due to the different dimensions and construction methods, there are some differences in network structure and inference results. The four groups of networks used for inference are labeled as overlapping construction generation network (OC-R), overlapping construction time network (OC-T), direct construction generation network (DC-R) and overlapping construction time network (OC-T). The statistical unit of the time state is minute, which best reflects the accuracy of network inference, so the inference results of 32 consecutive time states (more than 600 min) of the four groups of networks of different blast furnaces are selected to compare with the actual state, as shown in Figure 6, and the accuracy of the inference of the 32 consecutive states is recorded with the accuracy of the inference of all the 1400-min states in Table 1.

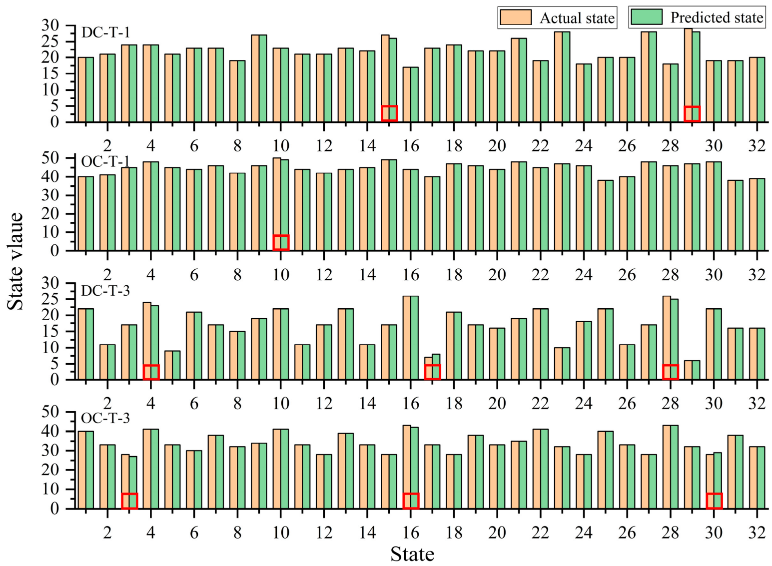

Figure 6. Reasoning results for 32 continuous time states. (The red boxes in the figure represent cases where the predicted state differs from the true state.).

Table 1. Accuracy statistics for generation state reasoning and time state reasoning.

Methods	Inference Accuracy of 32 Consecutive States	Average Accuracy	Methods	Inference Accuracy of 32 Consecutive States	Average Accuracy
OC-R-1	90.625%	84.375%	OC-T-1	93.75%	87.5%
DC-R-1	90.625%	87.5%	DC-T-1	96.875%	90.625%
OC-R-3	87.5%	81.25%	OC-T-3	90.625%	84.375%
DC-R-3	84.375%	78.125%	DC-T-3	90.625%	81.25%

As can be seen from Figure 7, the deviation of the inference results for each time state is within one minute, and the overall 32 consecutive time states' inference error is also within two minutes. Combined with Table 1, under the dimensions of interval generation and interval time, the average inference accuracies of two divisions satisfy the accuracy requirements of prediction, and the average inference accuracy decreases slowly when the inference length increases. The comparison of the inference accuracy in Table 1 shows that the inference accuracy of the training event set constructed directly in Blast Furnace 1 is higher, while the inference accuracy of the training event set constructed overlappingly in Blast Furnace 3 is higher.

The 1400-min generation prediction results under the direct construction of Blast Furnace No. 1 and the overlapping construction method of Blast Furnace No. 3 are selected for comparison with three improved machine learning methods, CNN-GRU, CNN-LSTM, and Attention-CNN. The first two comparative methods are based on the CNN network to perform the data feature extraction for the generation, and, respectively, they are performed by the GRU network and the LSTM network to perform the long-term prediction of generation, and the third method optimizes the process of feature extraction through the attention mechanism and uses the CNN network for long-term prediction of generation. The comparison methods all use the same batch size, number of training rounds, etc., and the generation data are divided into training set, validation set, and test set according to the ratio of 7:2:1. The prediction results of 1400 min for the four methods are shown in Figures 7 and 8.

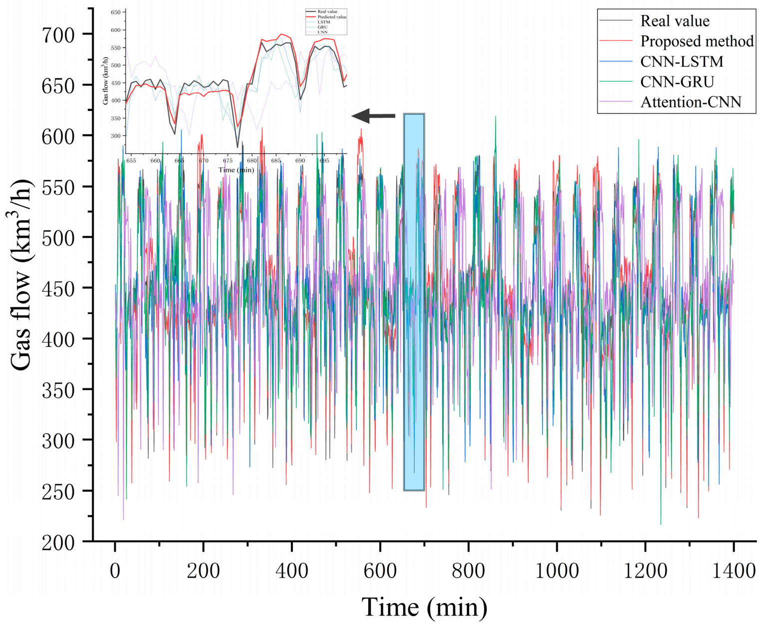

Figure 7. 1400 min predicted results of BFG generation for Blast Furnace 1. (The blue portion and subplot of the figure represent the randomly amplified detail portion of the 1400-min prediction results.).

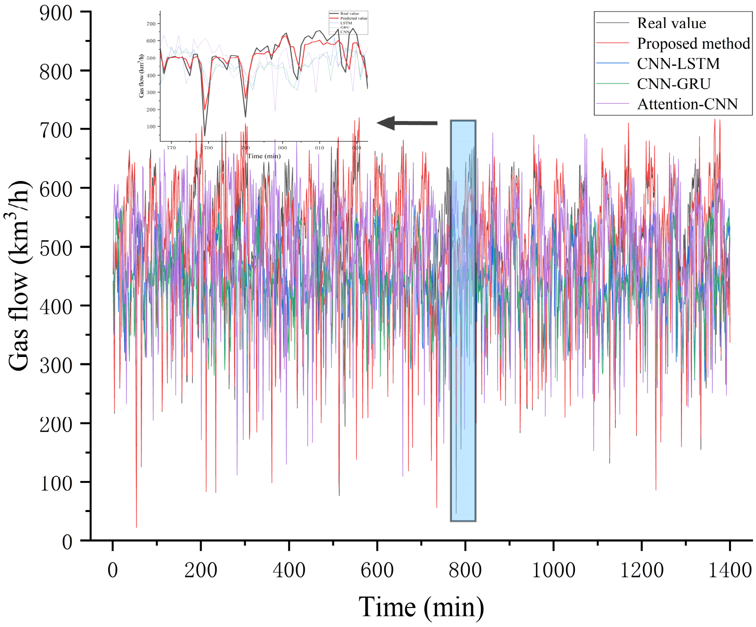

Figure 8. 1400 min predicted results of BFG generation for Blast Furnace 3. (The blue portion and subplot of the figure represent the randomly amplified detail portion of the 1400-min prediction results.).

As can be seen from the randomly zoomed in detail section of Figures 7 and 8, after a prediction length of 600 min the prediction results of this paper's method deviate less from the actual values as the prediction time increases, while the comparison algorithm prediction results deviate significantly.

In order to better assess the prediction effect of this paper's method, the mean absolute error (MAE), root mean square error (RMSE), and mean absolute percentage error (MAPE) are used as the evaluation indexes, and the calculation formulas of the three indexes are shown in Equations (16)–(18). The calculation results of the three indexes of this paper's method and comparison algorithm are recorded in Tables 2 and 3.

$$MAPE = \frac{100\%}{n}\sum_{i=1}^{n}\left|\frac{\hat{x}_i - x_i}{x_i}\right| \tag{16}$$

$$MAE = \frac{1}{n}\sum_{i=1}^{n}|\hat{x}_i - x_i| \tag{17}$$

$$RMSE = \sqrt{\frac{1}{n}\sum_{i=1}^{n}(\hat{x}_i - x_i)^2} \tag{18}$$

where, n is the number of test samples, $\hat{x}_i$ is the predicted value and x_i is the actual value.

Table 2. Comparison of 1400 min predicted effect of BFG generation for Blast Furnace 1.

Methods	MAE (km^3/h)	RMSE (km^3/h)	MAPE (%)
Proposed method	39.341	55.788	7.232
CNN-GRU	50.849	65.866	11.629
CNN-LSTM	56.796	70.625	13.257
Attention-CNN	84.588	96.184	23.972

Table 3. Comparison of 1400 min predicted effect of BFG generation for Blast Furnace 3.

Methods	MAE (km^3/h)	RMSE (km^3/h)	MAPE (%)
Proposed method	42.001	65.043	8.438
CNN-GRU	70.745	91.63	18.997
CNN-LSTM	76.626	96.982	20.349
Attention-CNN	90.028	109.19	25.848

Combining the three indexes in Tables 2 and 3, it can be seen that the three indexes of the prediction results of this paper's method are smaller than those of the comparison algorithms, showing higher prediction accuracy and smaller relative amount of error.

In order to evaluate the prediction results more comprehensively, this paper counts the cumulative errors of the prediction results of the four methods for Blast Furnace 1 and Blast Furnace 3 in comparison with the actual values, and the results will be shown in the Cumulative Distribution Function (CDF) plots, as in Figures 9 and 10.

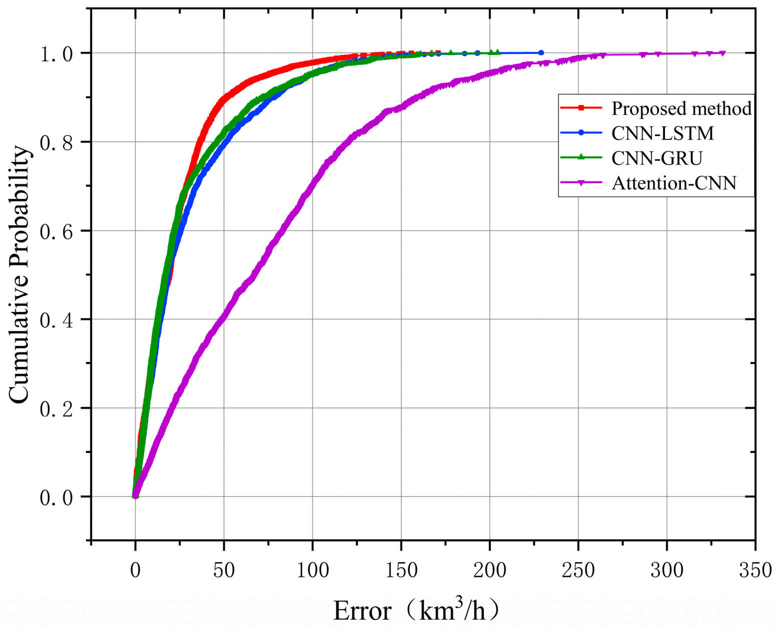

Figure 9. CDF plots of four prediction methods for Blast Furnace 1.

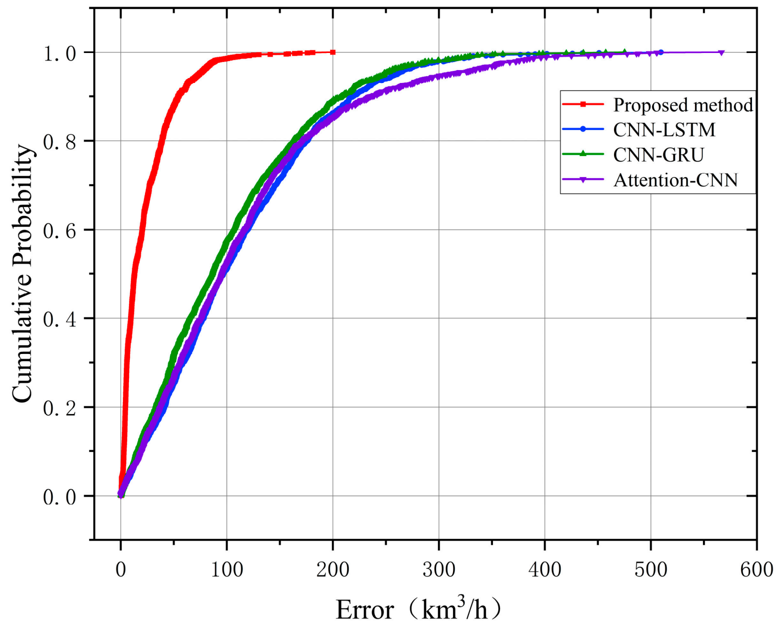

Figure 10. CDF plots of four prediction methods for Blast Furnace 3.

From Figures 9 and 10, it can be seen that the error distribution of this paper's method is concentrated in the interval of less than 100, and the 80% error between the predicted data and the real value is less than 40, and there is less long-tailed information, whereas the error interval of the comparative method is larger, and the long-tailed information is more, which demonstrates that this paper's model has a higher stability and the overall prediction accuracy. In addition, it can be seen through Figure 10 that the cumulative error of this paper's method for predicting the generation of No. 3 blast furnace is much smaller than the results of the comparison algorithm, and combined with the prediction results of No. 1 furnace, it can be concluded that the effectiveness of this paper's model for predicting the generation quasi-periods containing multi-segment hierarchical data.

5. Discussion

The prediction of the trend of BFG generation is very important for effective energy management in steel enterprises. This paper analyzes the mechanism and data of BFG generation and proposes a Bayesian network-based BFG generation prediction method, which has the advantage of utilizing the relationship between the blast furnace and its own hot blast furnace and obtaining the prediction state of BFG generation in two aspects through the inference of the Bayesian network. The experimental part compares the prediction results of this paper's method with those of three comparative algorithms for 1400 min, and the results show that this paper's method improves the prediction accuracy while demonstrating adaptability to the blast furnace data with multiple segments of grade data in the quasi-cycle.

The research in this paper is of some reference significance for the prediction of BFG generation, and some related improvement work is worth focusing on. In the future, adding nodes such as working situation in the network structure of the prediction model can refine the description of the BFG generation process and obtain a more accurate generation state by inference. In addition, there is still space for optimization in the division of the training event set in this paper, and it is worthwhile to conduct more in-depth research into how to improve the effect of network structure training by dividing the training event set, and how to make the training event set better describe the data relationship within the BFG generation.

Author Contributions: Conceptualization, Z.W. and D.W.; methodology, Z.W.; software, Z.W.; validation, Z.W.; formal analysis, Z.W. and D.W.; investigation, Z.W. and D.W.; resources, D.W.; data curation, Z.W.; writing—original draft preparation, Z.W.; writing—review and editing, D.W.; visualization, Z.W.; supervision, D.W.; project administration, D.W.; funding acquisition, D.W. All authors have read and agreed to the published version of the manuscript.

Funding: This research was funded by National Key Research and Development Program of China, grant number 2020YFB1711102.

Data Availability Statement: Restrictions apply to the availability of these data. Data were obtained from CHINA BAOWU STEEL GROUP CORPORATION LIMITED and are available from the authors with the permission of CHINA BAOWU STEEL GROUP CORPORATION LIMITED.

Conflicts of Interest: The authors declare no conflicts of interest. The funders had no role in the design of the study; in the collection, analyses, or interpretation of data; in the writing of the manuscript; or in the decision to publish the results.

Abbreviations

The following abbreviations are used in this manuscript:

BFG	Blast furnace gas
OC	Overlapping construction
DC	Direct construction
R	Generation network
T	Time network
OC-R	Overlapping construction generation network
OC-T	Overlapping construction time network
DC-R	Direct construction generation network
DC-T	Direct construction time network
MAE	Mean absolute error
RMSE	Root mean square error
MAPE	Mean absolute percentage error
CDF	Cumulative Distribution Function

References

1. E, D. Validation of CFD–DEM model for iron ore reduction at particle level and parametric study. *Particuology* **2020**, *51*, 163–172. [CrossRef]
2. Hou, Q.; E, D.; Kuang, S.; Li, Z.; Yu, A.J.P.T. DEM-based virtual experimental blast furnace: A quasi-steady state model. *Powder Technol.* **2017**, *314*, 557–566. [CrossRef]
3. Sun, W.; Wang, Q.; Zhou, Y.; Wu, J. Material and energy flows of the iron and steel industry: Status quo, challenges and perspectives. *Appl. Energy* **2020**, *268*, 114946. [CrossRef]
4. Pena, J.G.C.; de Oliveira, V.B.; Salles, J.L.F. Optimal scheduling of a by-product gas supply system in the iron- and steel-making process under uncertainties. *Comput. Chem. Eng.* **2019**, *125*, 351–364. [CrossRef]
5. Yang, L.; He, K.; Zhao, X.; Lv, Z. The prediction for output of blast furnace gas based on genetic algorithm and LSSVM. In Proceedings of the 2014 9th IEEE Conference on Industrial Electronics and Applications, Hangzhou, China, 9–11 June 2014; pp. 1493–1498.
6. Zhao, J.; Liu, Q.; Pedrycz, W.; Li, D. Effective Noise Estimation-Based Online Prediction for Byproduct Gas System in Steel Industry. *IEEE Trans. Ind. Inform.* **2012**, *8*, 953–963. [CrossRef]
7. Zhao, J.; Wang, W.; Liu, Y.; Pedrycz, W. A Two-Stage Online Prediction Method for a Blast Furnace Gas System and Its Application. *IEEE Trans. Control Syst. Technol.* **2011**, *19*, 507–520. [CrossRef]
8. Lv, Z.; Zhao, J.; Liu, Y.; Wang, W. Use of a quantile regression based echo state network ensemble for construction of prediction intervals of gas flow in a blast furnace. *Control Eng. Pract.* **2016**, *46*, 94–104. [CrossRef]
9. Sheng, C.; Zhao, J.; Wang, W.; Leung, H. Prediction Intervals for a Noisy Nonlinear Time Series Based on a Bootstrapping Reservoir Computing Network Ensemble. *IEEE Trans. Neural Networks Learn. Syst.* **2013**, *24*, 1036–1048. [CrossRef] [PubMed]
10. Liu, S.; Sun, W. Attention mechanism-aided data- and knowledge-driven soft sensors for predicting blast furnace gas generation. *Energy* **2023**, *262*, 125498. [CrossRef]

11. Sun, W.; Wang, Z.; Wang, Q. Hybrid event-, mechanism- and data-driven prediction of blast furnace gas generation. *Energy* **2020**, *199*, 117497. [CrossRef]
12. Zhao, J.; Han, Z.; Pedrycz, W.; Wang, W. Granular Model of Long-Term Prediction for Energy System in Steel Industry. *IEEE Trans. Cybern.* **2016**, *46*, 388–400. [CrossRef]
13. Han, Z.; Zhao, J.; Leung, H.; Wang, W. Construction of prediction intervals for gas flow systems in steel industry based on granular computing. *Control Eng. Pract.* **2018**, *78*, 79–88. [CrossRef]
14. Han, Z.; Pedrycz, W.; Zhao, J.; Wang, W. Hierarchical Granular Computing-Based Model and Its Reinforcement Structural Learning for Construction of Long-Term Prediction Intervals. *IEEE Trans. Cybern.* **2022**, *52*, 666–676. [CrossRef] [PubMed]
15. Wang, T.; Han, Z.; Zhao, J.; Wang, W. Adaptive Granulation-Based Prediction for Energy System of Steel Industry. *IEEE Trans. Cybern.* **2018**, *48*, 127–138. [CrossRef] [PubMed]
16. Zhao, J.; Wang, W.; Sun, K.; Liu, Y. A Bayesian Networks Structure Learning and Reasoning-Based Byproduct Gas Scheduling in Steel Industry. *IEEE Trans. Autom. Sci. Eng.* **2014**, *11*, 1149–1154. [CrossRef]
17. Li, J.; Hua, C.; Yang, Y.; Guan, X. Bayesian Block Structure Sparse Based T–S Fuzzy Modeling for Dynamic Prediction of Hot Metal Silicon Content in the Blast Furnace. *IEEE Trans. Ind. Electron.* **2018**, *65*, 4933–4942. [CrossRef]
18. Liu, Y.; Liu, Q.; Wang, W.; Zhao, J.; Leung, H. Data-driven based model for flow prediction of steam system in steel industry. *Inf. Sci.* **2012**, *193*, 104–114. [CrossRef]
19. Pan, Y.; Zhang, L.; Li, Z.; Ding, L. Improved Fuzzy Bayesian Network-Based Risk Analysis With Interval-Valued Fuzzy Sets and D–S Evidence Theory. *IEEE Trans. Fuzzy Syst.* **2020**, *28*, 2063–2077. [CrossRef]
20. Mann, H.B.J.E. Non-parametric tests against trend. *Econometrica* **1945**, *13*, 245. [CrossRef]
21. Box, G.E.P.; Cox, D.R. An Analysis of Transformations. *J. R. Stat. Soc. Ser. B (Methodol.)* **1964**, *26*, 211–243. [CrossRef]
22. Cooper, G.F.; Herskovits, E. A Bayesian Method for the Induction of Probabilistic Networks from Data. *Mach. Learn.* **1992**, *9*, 309–347. [CrossRef]